Cooperative Localization in VANETs: An Experimental Proof-of-Concept Combining GPS, IR-UWB Ranging and V2V Communications

Gia Minh Hoang[†#], Benoît Denis[†], Jérôme Härri[#], Dirk Slock[#]
[†]CEA-Leti, Minatec Campus, 17 rue des Martyrs, 38054 Grenoble, France
[#]EURECOM, SophiaTech Campus, 450 route des Chappes, 06904 Biot, France
E-mails: ghoang@enst.fr;benoit.denis@cea.fr;{haerri,slock}@eurecom.fr

***Abstract*—Future applications of Cooperative - Intelligent Transportation Systems (C-ITS) will require accurate and reliable localization capabilities in a variety of harsh operating contexts. In this paper, we account for proof-of-concept field validations of a cooperative localization approach suitable to GPS-enabled Vehicular Ad Hoc Networks (VANETs), which relies on Vehicle-to-Vehicle (V2V) communications (e.g., over ITS-G5) and Impulse Radio - Ultra Wideband (IR-UWB) V2V ranging measurements. First, we evaluate 1-D V2V ranging accuracy on a highway in real mobility conditions. Then, in the same environment, we evaluate the positive impact of cooperation on positioning (i.e., in comparison with standalone standard GPS) in the steady-state fusion regime. Finally, investigating the impact of erroneous initialization and full GPS denial conditions, we illustrate the resilience of the proposed solution, before discussing the limitations of the current evaluation setting.**

I. Introduction

In view of the demanding applications they are expected to support (e.g., highly autonomous driving, fleet coordination and control, advanced safety including vulnerable road users warning or protection...), Cooperative Intelligent Transport Systems (C-ITSs) will require very accurate and highly reliable positioning capabilities (i.e., consistent sub-meter accuracy, regardless of operating conditions), far beyond the current possibilities offered by satellite-based Global Positioning Systems (GPSs), especially in harsh environments such as urban canyons or intersections, tunnels... In this context, Cooperative Localization (CLoc) has been recently identified as a promising solution. Accordingly, mobile vehicles can assist each other by exchanging location-dependent information over Vehicle-to-Vehicle (V2V) communication links.

CLoc does not necessarily require V2V measurements in addition to V2V communications and on-board GPS data. In [1]–[3] for instance, GPS pseudoranges and optionally, vehicles motion information, are simply exchanged so that vehicles' relative positions can be estimated using a Particle Filter (PF) or a Weighted Least Squares (WLS) approach. Rather than sharing GPS pseudoranges, other studies reported in [4], [5] propose to broadcast GPS corrections, thus extending the principle of Differential GPS (DGPS) to dynamic reference base stations. However, all the previous techniques are strongly dependent on GPS availability. Moreover, they can only achieve accuracy levels of several meters at most. As another example, by sharing both GPS positions and pseudoranges over V2V links, cooperative map matching methods have also been put forward in [6], [7], where groups of vehicles are matched onto to a lane-level map. However, besides GPS availability issues, this technique depends on the Vehicular Ad hoc NETwork (VANET) topology. Finally, the Implicit Cooperative Positioning (ICP) approach, which relies on additional on-board sensing technologies (i.e., on top of V2V communications and GPS), aims at jointly estimating the positions of both sensing vehicles and sensed features in their vicinity (e.g., pedestrians, traffic lights, parked cars...) [8]. This technique can provide the required accuracy for a sufficient number of common detected features (typically, on the order of several tens), but it also necessitates quite expensive embedded sensors such as Light Detection And Ranging (LiDAR) devices, as well as complex decentralized data association and consensus algorithms so that sensing vehicles can agree on the detected features.

On the other hand, extensive research efforts have also been committed to make use of explicit V2V location-dependent radio measurements, as well as further information related to vehicle kinematics (e.g., speed, acceleration, heading, etc.) or a priori road maps. In [9], a simplified CLoc fusion architecture based on an Extended Kalman Filter (EKF) combines GPS data with V2V range measurements in a star topology (thus, avoiding the exchange of range vectors). Another integrated fusion architecture based on a modified cubature KF in [10] fuses GPS data with both V2V ITS-G5 Doppler shifts and ranges. In [11], the GPS data is fused with the Received Signal Strength Indicator (RSSI) of V2V messages such as ITS-G5 Cooperative Awareness Messages (CAMs), with inertial sensor data from driver's smartphone and a priori map information. A two-step Bayesian framework has been proposed, including an Unscented Kalman Filter (UKF) in charge of pre-processing the inertial-based heading, whereas a core PF is used to fuse all the remaining sources of information. Real-world experiments have even been conducted in the city of Porto. In another similar solution referred to as Virtual Anchors assisted CLoc (VA-CLoc) [12]–[16], each vehicle considers its

978-1-5386-6436-0/18/$31.00

neighbors as potential "Virtual Anchors" (i.e., mobile anchors with approximate knowledge of their own positions). First, all vehicles piggyback their latest absolute positions in beacons, which are sent over V2V communication links (e.g., ITS-G5 CAMs again). Various cooperative formulations of both EKF and PF have thus been considered at the "Ego"[1] vehicle to fuse on-board GPS data with V2V range-dependent radio information (see Fig. 1). Finally, each vehicle contributes to improve the localization of its neighbors by broadcasting in return its own fusion results in subsequent beacons. In terms of incorporated V2V radio measurements, the RSSI associated with received CAMs has also been considered for simplicity in [12]–[14]. Preliminary experimental validations in a highway scenario [17] have shown significant gains in comparison with standard GPS performance (e.g., reducing the 2-D location error by 50% in average). However, none of the solutions above could meet the targeted accuracy of 1 m.

More recently, accurate V2V range measurements based on Impulse Radio - Ultra Wideband (IR-UWB) Round Trip - Time of Flight (RT-ToF) estimation have been incorporated in the problem, instead of using ITS-G5 RSSI metrics, while keeping ITS-G5 uniquely for V2V communications. Even more promising gains have been shown by means of simulations in pathological cases such as narrow streets or GPS-altered environments [15], [16]. However, to the best of our knowledge, only rare real field trials have been conducted so far with V2V IR-UWB range measurements. In [18], aiming at improving the horizontal positioning accuracy in a group of three vehicles, DGPS pseudoranges have been fused with V2V IR-UWB range measurements and bearing measurements using an EKF in different scenarios. However, these preliminary tests have shown that the combination of DGPS with IR-UWB could be occasionally counterproductive, or even worse than stand-alone DGPS. Timing errors corrupting the IR-UWB data have been incriminated as a plausible reason. The discrepancy between large prior positioning errors and very accurate ranging observations could also lead to violate the usual operating conditions of EKF (or PF), as illustrated in [15]. Besides, the fusion between IR-UWB and standard mass-market GPS has not been investigated yet (but mostly with DGPS).

In this paper, we account for new field trials and offline proof-of-concept validations of the VA-CLoc approach, relying on a demonstration platform developed in the frame of the HIGHTS project [19]. On this occasion, we first evaluate the 1-D precision of IR-UWB V2V range measurements under mobility. We then illustrate performance gains achieved in terms of positioning beyond standard GPS in the nominal steady-state fusion regime (i.e., with reliable initialization and reliable information from neighboring vehicles), before investigating the particular effects of erroneous initialization and full GPS denial at the "Ego" vehicle.

The remainder of the paper is organized as follows. In Section II, we recall the cooperative localization problem formulation, as well as the proposed VA-CLoc solution. In Section III, we describe the experimental setting and the tested scenario. Then in Section IV, we present the corresponding offline validation results, before discussing their current limitations in Section V. Finally, Section VI concludes the paper.

[1]The so-called "Ego" vehicle herein performs fusion at a given point in time. Given the decentralized nature of VA-CLoc, it shall be understood that the roles are interchangeable with Virtual Anchors over time.

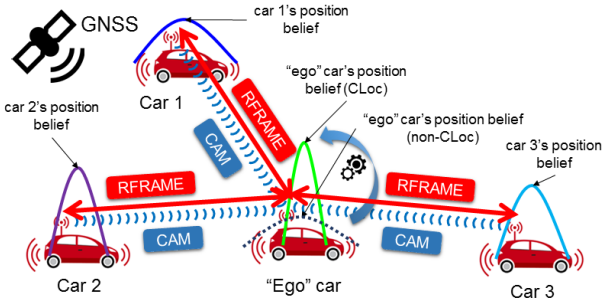

Fig. 1. Illustration of VA-CLoc principle: The "Ego" car performs data fusion after receiving ITS-G5 V2V CAM messages and exchanging IR-UWB V2V ranging frames (FRAME) with respect to single-hop "Virtual Anchors".

II. Problem Formulation and Proposed Algorithm

A. Cooperative Localization in VANETs

We consider a VANET of several vehicles cooperating over V2V ITS-G5 links. The goal of the so-called "Ego" vehicle is thus to infer its position (as part of its so-called "state" in the following) based on its own estimated GPS position, on V2V IR-UWB range measurements with respect to its single-hop neighbors, as well as on imperfect state information received from these neighbors, which are viewed as "Virtual Anchors" (i.e., encapsulating estimated locations and related uncertainties in V2V ITS-G5 CAMs) (See Fig. 1).

B. Overall System Model

The state vector of vehicle i includes its 2-D coordinates $\mathbf{x}_{i,k} = (x_{i,k}, y_{i,k})^\dagger$ and velocities $\mathbf{v}_{i,k} = (v^x_{i,k}, v^y_{i,k})^\dagger$, all expressed at discrete time step k according to a local timeline[2].

1) Mobility Model: We first consider a generic discrete-time 2-D mobility model, as follows:

$$\mathbf{x}_{i,k+1} = \mathbf{A}\mathbf{x}_{i,k} + \mathbf{B}(\Delta T)\mathbf{v}_{i,k} + \mathbf{C}(\Delta T)\mathbf{w}_{i,k}, \qquad (1)$$

where $\mathbf{A} = \mathbf{I}_2$, $\mathbf{B}(\Delta T) = \Delta T \mathbf{I}_2$, $\mathbf{C}(\Delta T) = \frac{\Delta T^2}{2}\mathbf{I}_2$, $\mathbf{I}_2$ the identity matrix of size 2×2, ΔT the time step, $\mathbf{w}_{i,k} = (w^x_{i,k}, w^y_{i,k})^\dagger \sim \mathcal{N}((0,0)^\dagger, \mathbf{Q}_{i,k})$ the 2-D process noise vector and $\mathbf{Q}_{i,k}$ the related covariance. This model is used to predict and resynchronize "Ego" and neighbors' locations.

2) Observation Model:

a) GPS Absolute Position: The 2-D estimated GPS position, $\mathbf{x}^{\text{GPS}}_{i,k} = (z^x_{i,k}, z^y_{i,k})^\dagger$, is affected by an additive noise term $\mathbf{n}^{\text{GPS}}_{i,k} = (n^x_{i,k}, n^y_{i,k})^\dagger$, which is assumed to be i.i.d. centered Gaussian [20] with standard deviation σ_{GPS}, as follows:

$$z^x_{i,k} = x_{i,k} + n^x_{i,k}, \quad z^y_{i,k} = y_{i,k} + n^y_{i,k}. \qquad (2)$$

b) IR-UWB V2V Ranges: Through a cooperative ranging protocol (e.g., based on Time of Arrival (ToA) estimation and multi-way handshake transactions), node i can estimate the V2V distance $z_{j\to i,k}$ with respect to node j:

$$z_{j\to i,k} = \|\mathbf{x}_{i,k} - \mathbf{x}_{j,k_i}\| + n_{j\to i,k}, \qquad (3)$$

[2]Due to asynchronously sampled time instants, the index k is different from one vehicle to others. The subscript of the "Ego" is herein dropped for brevity.

Algorithm 1 EKF-based Fusion (iteration k, "ego" vehicle i)

1: **CAM Collection:** Receive CAMs from the set $\mathcal{S}_{\to i,k}$ of perceived neighbors, extract the Gaussian beliefs $\{\widehat{\mathbf{x}}_{j,k}, \mathbf{P}_{j,k}\}$, the velocity $\mathbf{v}_{j,k}$, the timestamps $t_{j,k}$ and (optionally) mobility parameters like $\mathbf{Q}_{j,k}$, $j \in \mathcal{S}_{\to i,k}$.

2: **Prediction and Data Synchronization:** Perform prediction of both "ego" and neighboring beliefs based on mobility prediction models at the "ego" estimation instant $t_{i,k}$

$$\begin{aligned}
\widehat{\mathbf{x}}_{i,k|k-1} &= \mathbf{A}\mathbf{x}_{i,k-1} + \mathbf{B}(\Delta T)\mathbf{v}_{i,k-1},\\
\mathbf{P}_{i,k|k-1} &= \mathbf{A}\mathbf{P}_{i,k-1}\mathbf{A}^{\dagger} + \mathbf{C}(\Delta T)\mathbf{Q}_{i,k}\mathbf{C}(\Delta T)^{\dagger},\\
\mathbf{x}_{j,k_i|k} &= \mathbf{A}\mathbf{x}_{j,k} + \mathbf{B}(\Delta T_k^{i,j})\mathbf{v}_{j,k},\\
\mathbf{P}_{j,k_i|k} &= \mathbf{A}\mathbf{P}_{j,k}\mathbf{A}^{\dagger} + \mathbf{C}(\Delta T_k^{i,j})\mathbf{Q}_{j,k}\mathbf{C}(\Delta T_k^{i,j})^{\dagger},\\
\Delta T_k^{i,j} &= t_{i,k} - t_{j,k}, \quad j \in \mathcal{N}_{\to i,k}.
\end{aligned}$$

3: **Correction:** Aggregate the predicted states $\widehat{\mathbf{x}}_{j,k_i|k}$ and covariance matrices $\mathbf{P}_{j,k_i|k}$, $j \in \mathcal{S}_{\to i,k}$ (by constructing block diagonal matrix) to obtain $\widehat{\mathbf{x}}_{\mathcal{S}\to i,k|k-}$ and $\mathbf{P}_{\mathcal{S}\to i,k|k-}$ respectively then

$$\begin{aligned}
\widehat{\mathbf{x}}_{i\cup\mathcal{S},k|k-} &= (\widehat{\mathbf{x}}_{i,k|k-1}^{\dagger}, \widehat{\mathbf{x}}_{\mathcal{S}\to i,k|k-}^{\dagger})^{\dagger},\\
\mathbf{P}_{i\cup\mathcal{S},k|k-} &= \begin{pmatrix} \mathbf{P}_{i,k|k-1} & \mathbf{0} \\ \mathbf{0} & \mathbf{P}_{\mathcal{S}\to i,k|k-} \end{pmatrix},\\
\mathbf{H}_{i,k} &= \left.\frac{\partial \mathbf{h}_{i,k}}{\partial \mathbf{x}_{i\cup\mathcal{S},k}}\right|_{\mathbf{x}_{i\cup\mathcal{S},k}=\widehat{\mathbf{x}}_{i\cup\mathcal{S},k|k-}},\\
\mathbf{K}_{i,k} &= \mathbf{P}_{i\cup\mathcal{S},k|k-}\mathbf{H}_{i,k}^{\dagger}(\mathbf{H}_{i,k}\mathbf{P}_{i\cup\mathcal{S},k|k-1}\mathbf{H}_{i,k}^{\dagger} + \mathbf{R}_{i,k})^{-1},\\
\widehat{\mathbf{x}}_{i\cup\mathcal{S},k} &= \widehat{\mathbf{x}}_{i\cup\mathcal{S},k|k-} + \mathbf{K}_{i,k}(\mathbf{z}_{i,k} - \mathbf{h}_{i,k}(\widehat{\mathbf{x}}_{i\cup\mathcal{S},k|k-})),\\
\mathbf{P}_{i\cup\mathcal{S},k} &= (\mathbf{I} - \mathbf{K}_{i,k}\mathbf{H}_{i,k})\mathbf{P}_{i\cup\mathcal{S},k|k-},\\
\widehat{\mathbf{x}}_{i,k} &= [\widehat{\mathbf{x}}_{i\cup\mathcal{S},k}]_{1:2}, \quad \mathbf{P}_{i,k} = [\mathbf{P}_{i\cup\mathcal{S},k}]_{1:2,1:2}.
\end{aligned}$$

4: **Belief Encapsulation and Broadcast:** Encapsulate the fused belief $\{\widehat{\mathbf{x}}_{i,k}, \mathbf{P}_{i,k}\}$, the velocity measurement $\mathbf{v}_{i,k}$, and its timestamp $t_{i,k}$ in a CAM and broadcast.

where $n_{j\to i,k}$ is an i.i.d. centered Gaussian noise term with standard deviation σ_{UWB}.

We depict the stacked states of "Virtual Anchors" as $\mathbf{x}_{\mathcal{S}\to i,k} = \{\mathbf{x}_{j,k_i} | \forall j \in \mathcal{S}_{\to i,k}\}$, the augmented state as $\mathbf{x}_{i\cup\mathcal{S},k} = (\mathbf{x}_{i,k}^{\dagger}, \mathbf{x}_{\mathcal{S}\to i,k}^{\dagger})^{\dagger}$, the vector of V2V ranges as $\mathbf{z}_{\mathcal{S}\to i,k} = \{z_{j\to i,k} | \forall j \in \mathcal{S}_{\to i,k}\}$, and the full observation vector as:

$$\mathbf{z}_{i,k} = (\mathbf{x}_{i,k}^{\text{GPS}\dagger}, \mathbf{z}_{\mathcal{S}\to i,k})^{\dagger} = \mathbf{h}_{i,k}(\mathbf{x}_{i\cup\mathcal{S},k}) + \mathbf{n}_{i,k}, \tag{4}$$

where $\mathbf{h}_{i,k}(\cdot)$ and $\mathbf{n}_{i,k}$ represent the mixed linear/nonlinear function of the augmented state and the measurement noise, respectively. Assume the distinct measurement noises are independent, the noise covariance matrix is given by:

$$\mathbf{R}_{i,k} = \begin{pmatrix} \sigma_{\text{GPS}}^2\mathbf{I}_2 & \mathbf{0} \\ \mathbf{0} & \sigma_{\text{UWB}}^2\mathbf{I}_{|\mathcal{S}\to i,k|} \end{pmatrix}. \tag{5}$$

C. EKF-based Fusion

In our data fusion context, since observations are partly nonlinear with respect to the state variables, we consider a simple EKF-based Bayesian data fusion framework (See Algorithm 1). Vehicle i's state belief at time t (i.e., $t_{i,k}$), which is assumed to be multivariable Gaussian, is thus represented by the mean $\hat{\mathbf{x}}_{i,k}$ and its associated covariance $\mathbf{P}_{i,k}$.

III. Experimental Setting and Tested Scenario

Field trials took place at Tass' vehicular test facilities in Helmond, Netherlands, in Dec. 2017. These tests were relying on a physical proof-of-concept platform integrated in the frame of the HIGHTS project [19], consisting of 3 equipped vehicles forming a platoon (See Fig. 2). These vehicles made several rounds along the A270/N270 highway section. The followed route deliberately included a combination of straight and curvy portions of road for better representativity and more realistic performance assessment.

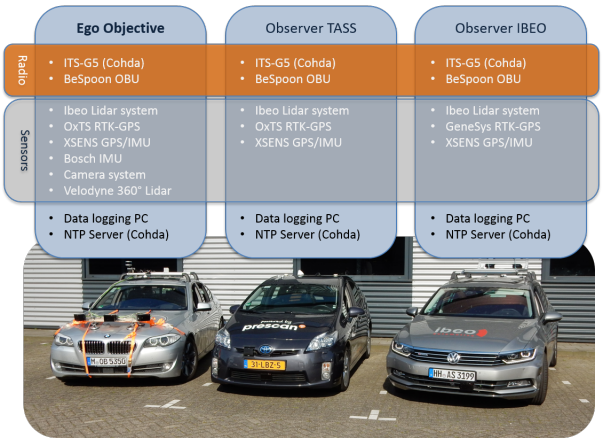

Fig. 2. Three vehicles involved in the proof-of-concept field tests, along with their embedded technologies.

Objective's car was considered as the "Ego" vehicle under test, endowed with a standard GPS (embedded in its on-board Cohda MK5 box). On the other hand, Tass' and Ibeo's vehicles were playing the roles of assisting vehicles (i.e., virtual anchors according to VA-CLoc), broadcasting their own Real Time Kinematics (RTK) or/and standard GPS information (issued by the Lidar sub-system in the latter case) over the ITS-G5 V2V channel. Thus, various combinations could be tested in terms of both the number of cooperative neighbors and their GPS quality.

The ground truth position of the "Ego" vehicle (i.e., the reference position used for performance evaluation) has been computed through a complex graph-based Simultaneous Localization and Mapping (SLAM) fusion algorithm, combining on-board RTK GPS data, LiDAR scans and odometry data.

During these experiments, standard GPS data were available at the "Ego" vehicle at the rate of 30 Hz. So as to limit the impact of over-oscillations (and frequent outliers/spikes) affecting these measurements, a pre-smoothing step using a sliding window of 0.2 s was applied before feeding the observation vector of the fusion filter. The ITS-G5 CAMs issued at the Cohda MK5 box (i.e., encapsulating GPS or RTK information from the two neighboring vehicles) were received at the "Ego" vehicle at the average rate of 10 Hz. For higher fusion rates (i.e., between consecutive reception events), we could rely on mobility-based predictions to update these neighbors' positions.

Besides, peer-to-peer ranging transactions were performed between the three cars, relying on BeSpoon's IR-UWB devices [21]. In particular, two range measurements with respect to Tass' and Ibeo's vehicles were made available at Objective's car at the rate of 10 Hz and injected into the observation vector of the fusion filter (i.e., besides standard GPS readings). However, due to the relative instability of these ranging

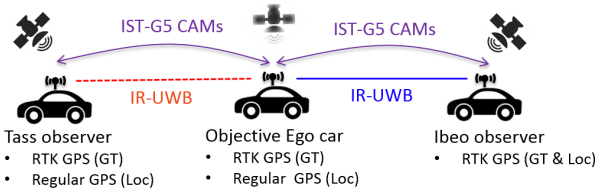

Fig. 3. Physical deployment scenario considered for both V2V ranging and V2V-aided cooperative localization testing on the field.

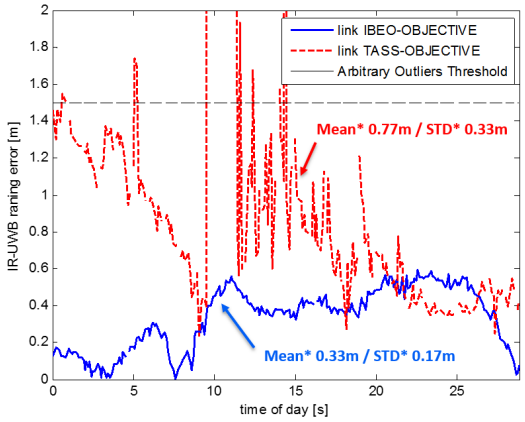

Fig. 4. RT-ToF based ranging errors as a function of time over two distinct V2V IR-UWB links (btw. "Ego" vehicle and cooperating neighbors); Empirical statistics are drawn over samples below the arbitrary outliers detection threshold (i.e., 1.5m in the shown example).

measurements under typical vehicular mobility (See IV-A), one simple threshold-based outliers rejection mechanism had to be implemented in the filter before performing fusion.

All in all, given the available refreshment rates and the constraints of the various input data, the best fusion rate was set to 10 Hz. For the sake of performance evaluation, representative portions of the overall test drive trajectory have been selected, lasting for approximately 30 sec each, where all the desired modalities cited above were simultaneously available and sufficiently consistent.

IV. Offline Validation Results

A. IR-UWB V2V Ranging

Relying on the IR-UWB devices embedded in the ranging sub-system of the integrated platform, we first evaluate the performance of V2V ranging based on RT-ToF estimation independently. For this evaluation, we consider the same deployment scenario as that used for cooperation, illustrated on Fig. 3. In the following, note that the collected range measurements are reused as observations to feed the VA-CLoc fusion algorithm running at the "Ego" vehicle. Fig. 4 shows the ranging estimation error as a function of time at Objective's "Ego" vehicle over one of the selected portions of trajectory, with respect to the two neighboring vehicles. It is thus demonstrated that submetric V2V ranging accuracy can be met under practical mobility conditions, typically with a mean error equal to 0.33 m and an error standard deviation of 0.17 m with respect to Ibeo's vehicle (resp. 0.77 m and 0.33 m, with respect to Tass' vehicle).

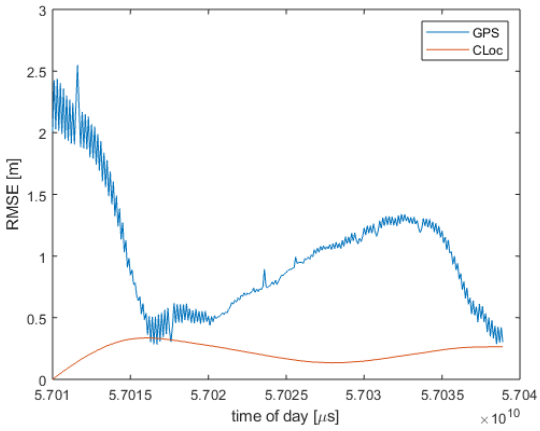

Fig. 5. 2-D location error at Objective's car as a function of time along the selected portion of trajectory, for Cohda box's GPS (blue) and VA-CLoc fusion with Ibeo's car's RTK and V2V IR-UWB range measurements (red) (1 virtual anchor), in the steady-state fusion regime.

B. Cooperative Localization in the Steady-State Regime

One step ahead, the idea is now to evaluate the performance of VA-CLoc localization. For this sake, we first partially rely on the deployment scenario of Fig. 3, where cooperation is intended with respect to Ibeo's vehicle only, assuming a steady-state fusion regime (i.e., assuming the convergence of cooperative localization prior to the initial timestamp). The "Ego" vehicle thus benefits from a reliable initial guess on the one hand (i.e., its own local RTK for the very first iteration, before using its standard GPS for the rest of the trajectory), while the assisting car broadcasts reliable RTK information on the other hand (e.g., assuming prior VA-CLoc convergence also on the neighbor's side).

Fig. 5 shows the corresponding 2-D location RSME as a function of time over the same selected portions of trajectory as before, for (i) "Ego" vehicle's standard GPS and (ii) VA-CLoc after fusing the latter GPS data with Ibeo car's RTK data received over ITS-G5 CAMs and IR-UWB ranges. Fig. 6 shows the empirical CDF of this 2-D location error over the full trajectory. In this illustrative example, the performance gain achieved through VA-CLoc is already rather spectacular, leading to a 2-D location error that is almost constant in the steady-state regime, spanning between 0.2 m (median) and 0.3 m (worst case), even when the standalone GPS error is up to 1.3 m - 2 m. Hence, Objective's vehicle gets clear benefits (at least to a significant extent) from both the presence of a neighboring vehicle with reliable information in its vicinity and accurate range measurements with respect to this neighbor.

C. Cooperative Localization under Erroneous Initialization and/or Full GPS Denial

The goal is now to evaluate the effects of imperfect initialization (i.e., what we also call "Cold Start" herein), as well as of a varying reliability/number of assisting neighbors (i.e., assuming one additional but less reliable neighbor) and finally, of full GPS denial at the "Ego" vehicle (i.e., emulating deliberately GPS loss for 10 sec).

Fig. 7 shows the 2-D location RSME as a function of time over the same trajectory as previously, for "Ego" vehicle's

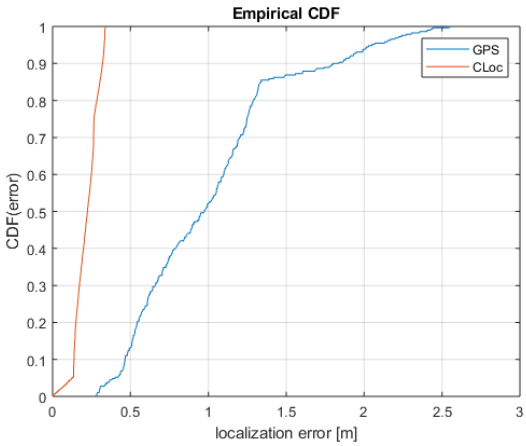

Fig. 6. Empirical CDF of 2-D location error at Objective's car along the selected portion of trajectory, for Cohda box's GPS (blue) and VA-CLoc fusion with Ibeo's car's RTK and V2V IR-UWB range measurements (red) (1 virtual anchor), in the steady-state fusion regime.

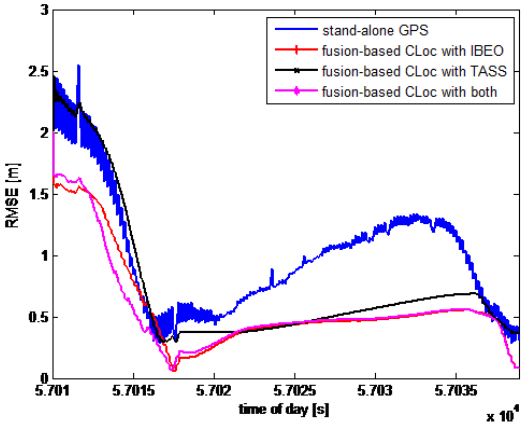

Fig. 7. 2-D location error at Objective's car as a function of time along the selected portion of trajectory, for Cohda box's GPS (blue) or VA-CLoc fusion with V2V IR-UWB range measurements and Ibeo's car's RTK only (red), Tass' Cohda box's GPS only (black) or both neighboring cars (magenta) (i.e., up to 2 virtual anchors), assuming a "cold start" at Objective's "Ego" car (i.e., initial guess based on Cohda box's GPS).

standard GPS and VA-CLoc after fusing the latter GPS data with IR-UWB ranges and Ibeo car's RTK data and/or Tass car's standard GPS data received over ITS-G5 CAMs, while assuming initialization through standard GPS at the "Ego" vehicle. The first remark is that one single GPS-enabled neighbor (i.e., Tass) already enables to boost performance in comparison with standalone GPS once the steady-state fusion regime is reached, with a maximum error of about 0.6m at the "Ego" (after convergence), whereas one single RTK-enabled neighbor (Ibeo) provides an even lower maximum error below 0.5m (still after convergence). Finally, relying on both assisting neighbors provides mostly faster convergence in the initial phase (i.e., when starting from scratch before convergence). On Fig. 8, as a complementary result, we note almost no performance degradation under temporary full GPS denial at the "Ego" after convergence (for more than 10 sec), then showing the resilience of the proposed solution. Overall, these VA-CLoc validation results confirm the capability of V2V-aided cooperative localization to provide not only an accuracy

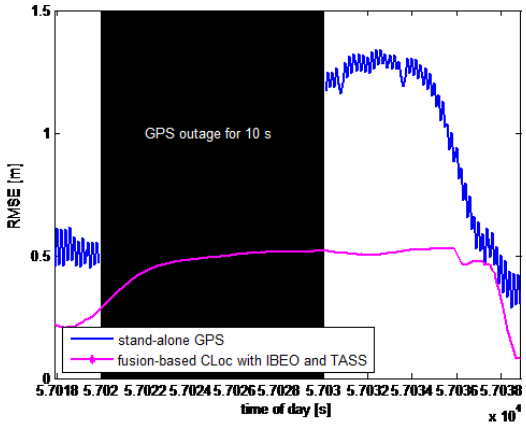

Fig. 8. 2-D location error at Objective's car as a function of time along the selected portion of trajectory, for Cohda box's GPS (blue) or VA-CLoc fusion with V2V IR-UWB range measurements, Ibeo's car's RTK and Tass' Cohda box's GPS (magenta) (i.e., 2 virtual anchors) in the steady-state fusion regime, assuming temporary full GPS denial at Objective's "Ego" car (black area).

of 0.25 m in > 70 % of time, but also a constant quality of service, robust against standard GPS impairments.

V. Discussion

A. Limitations of Collected Field Data

The V2V IR-UWB ranging errors observed under typical vehicular mobility (i.e., highway mobility) were more erratic than expected (i.e., with large transient errors of several meters occasionally on the link with respect to Tass' vehicle). Other V2V ranging tests realized under moderate vehicular mobility were more successful and compliant with the accuracy level obtained over the other link with respect to Ibeo's vehicle (i.e., with errors on the order of a few 10s of cm, as expected). Even if IR-UWB is still much more favourable than RSSI to account for V2V range information (e.g., [17]), these unexpectedly large errors alter the VA-CLoc filtering capabilities, by limiting the efficiency of observation-based corrections (after outliers rejection) or by introducing extra observation noise. This phenomenon may result from erroneous synchronization procedures (e.g., wrong positioning of ToA search windows), mobility-induced relative drifts, or delayed ToA estimates based on secondary multipath components. More robust synchronization and/or ToA estimation procedures shall be implemented to better support high mobility regimes.

As for the "Ego" vehicle's state prediction, since the time basis of the on-board Inertial Measurement Unit (IMU) could not overlap that of the RTK (due to some technical problems occurred during the data logging phase), the latter RTK was indirectly used to determine vehicle's speed and heading information (rather than relying on on-board sensors such as the wheel speed sensor and the gyroscope, as scheduled initially), while operating on a portion where RTK could still be used for ground truth.

Finally, the actual uncertainty of both standard GPS and range measurements were not provided during the experiments, thus leading us to make guesses based on rather strong and possibly unfavorable a priori statistical assumptions.

B. Limitations of Current Algorithmic Implementation

In the implemented version of VA-CLoc, the state of cooperative neighbors is predicted at the "Ego" vehicle based on a simplistic a priori mobility model, whereas the state of the "Ego" vehicle it-self can rely either on the same kind of models or alternatively, on its on-board IMU. In environments naturally generating erratic mobility (typically urban intersections), there could be a significant mismatch between a priori mobility models and actual mobility patterns. Thus, a generalized usage of on-board sensor information (possibly by encapsulating the related information in the CAM too) would be clearly beneficial. Besides, if an "Ego" vehicle can always use its own on-board IMU, which naturally provides high rate measurements, the collected neighbors' mobility information might be less reliable due to the reception of CAM updates at much lower rates (than that of the local IMU). In other words, while waiting for enough CAMs to perform VA-CLoc, if the neighbors move erratically, predictions based on the latest available CAMs are prone to larger errors. Thus, the prediction covariance terms should ideally be adjusted to avoid biases propagation.

Finally, the current VA-CLoc implementation can be easily extended to integrate the lane width or even the relative position of the vehicle with respect to the lane borders (e.g., based on a camera), thus improving further the performance (e.g., by adding mathematical constraints to the posterior density of the estimated state, similarly to the PF implementation in [15]).

VI. Conclusion

In this paper, relying on field data collected on a portion of highway, we have provided offline proof-of-concept validations of a cooperative localization algorithm suitable to VANETs. Accordingly, one "Ego" vehicle fuses its own embedded GPS data with accurate V2V ranges measured with respect to neighboring vehicles, which also broadcast their own position estimates over ITS-G5 V2V communication links. This algorithm benefits from V2V cooperation to achieve quasi-constant localization accuracy around 0.25 m, in compliance with most short- to medium-term vehicular applications, without being sensitive to large GPS errors above 2 m. These results thus confirm the capability of V2V-aided cooperative localization to improve both accuracy and small-scale service resilience. Depending on the operating context however (in terms of on-board technologies, connectivity, environment…) and application requirements, the proposed VA-CLoc approach could be advantageously replaced by - or combined with- other algorithms (e.g., relying on more costly embedded technologies such as LiDARs [8] or on vehicle-to-infrastructure communications). Thus, the definition of context-switching decision rules to select the optimal fusion strategy at any time/place [22] is expected to enable even larger-scale continuity of the localization service.

Acknowledgment

This work has been performed in the frame of the *HIGHTS* project, which is funded by the European Commission (636537-H2020). The authors would like to warmly thank their colleagues in charge of the proof-of-concept platform integration and field trials, and more particularly, Marcus Bartels from Ibeo Automotive Systems GmbH. Besides, EURECOM also acknowledges the support of its industrial members, namely, BMW Group, IABG, Monaco Telecom, Orange, SAP, ST Microelectronics, and Symantec.

References

[1] E. Richter, M. Obst, R. Schubert, and G. Wanielik, "Cooperative Relative Localization using Vehicle-to-Vehicle Communications," in *Proc. FUSION'09*, pp. 126–131, July 2009.

[2] N. Alam, A. Balaei, and A. G. Dempster, "Relative Positioning Enhancement in VANETs: A Tight Integration Approach," *IEEE Trans. on ITS*, vol. 14, pp. 47–55, March 2013.

[3] K. Liu, H. B. Lim, E. Frazzoli, H. Ji, and V. Lee, "Improving Positioning Accuracy Using GPS Pseudorange Measurements for Cooperative Vehicular Localization," *IEEE Trans. on VT*, vol. 63, pp. 2544–2556, July 2014.

[4] M. Rohani, D. Gingras, and D. Gruyer, "Dynamic Base Station DGPS for Cooperative Vehicle Localization," in *Proc. ICCVE'14*, Nov. 2014.

[5] K. Lassoued, P. Bonnifait, and I. Fantoni, "Cooperative Localization with Reliable Confidence Domains Between Vehicles Sharing GNSS Pseudoranges Errors with No Base Station," *IEEE ITS Mag.*, vol. 9, no. 1, pp. 22–34, 2017.

[6] N. Mattern, M. Obst, R. Schubert, and G. Wanielik, "Cooperative Vehicle Localization Algorithm - Evaluation of the CoVeL Approach," in *Proc. SSD'12*, pp. 1–5, March 2012.

[7] M. Rohani, D. Gingras, and D. Gruyer, "A Novel Approach for Improved Vehicular Positioning Using Cooperative Map Matching and Dynamic Base Station DGPS Concept," *IEEE Trans. on ITS*, vol. 17, pp. 230–239, Jan. 2016.

[8] G. Soatti, M. Nicoli, N. Garcia, B. Denis, R. Raulefs, and H. Wymeersch, "Implicit Cooperative Positioning in Vehicular Networks," *IEEE Trans. on ITS*, vol. PP, no. 99, pp. 1–17, 2018.

[9] M. Rohani, D. Gingras, V. Vigneron, and D. Gruyer, "A New Decentralized Bayesian Approach for Cooperative Vehicle Localization Based on Fusion of GPS and VANET Based Inter-Vehicle Distance Measurement," *IEEE ITS Mag.*, vol. 7, no. 2, pp. 85–95, 2015.

[10] J. Liu, B. Cai, and J. Wang, "Cooperative Localization of Connected Vehicles: Integrating GNSS With DSRC Using a Robust Cubature Kalman Filter," *IEEE Trans. on ITS*, vol. 18, pp. 2111–2125, Aug. 2017.

[11] S. Cruz, T. Abrudan, Z. Xiao, N. Trigoni, and J. Barros, "Neighbor-Aided Localization in Vehicular Networks," *IEEE Trans. on ITS*, vol. 18, pp. 2693–2702, Oct. 2017.

[12] G. Hoang, B. Denis, J. Härri, and D. Slock, "Breaking the Gridlock of Spatial Correlations in GPS-Aided IEEE 802.11p-based Cooperative Positioning," *IEEE Trans. on VT*, vol. 65, pp. 9554–9569, Dec. 2016.

[13] G. Hoang, B. Denis, J. Härri, and D. Slock, "On Communication Aspects of Particle-based Cooperative Positioning in GPS-Aided VANETs," in *Proc. IV'16 - CCP Workshop*, pp. 20–25, June 2016.

[14] G. Hoang, B. Denis, J. Härri, and D. Slock, "Select Thy Neighbors: Low Complexity Link Selection for High Precision Cooperative Vehicular Localization," in *Proc. IEEE VNC'15*, pp. 36–43, Dec. 2015.

[15] G. Hoang, B. Denis, J. Härri, and D. Slock, "Mitigating Unbalanced GDoP Effects in Range-Based Vehicular Cooperative Localization," in *Proc. IEEE ICC'17 - ICC Workshops*, pp. 659–664, May 2017.

[16] G. Hoang, B. Denis, J. Härri, and D. Slock, "Robust and Low Complexity Bayesian Data Fusion for Hybrid Cooperative Vehicular Localization," in *Proc. IEEE ICC'17*, pp. 1–6, May 2017.

[17] S. Severi, H. Wymeersch, J. Härri, M. Ulmschneider, B. Denis, and M. Bartels, "Beyond GNSS: Highly Accurate Localization for Cooperative-Intelligent Transport Systems," in *Proc. IEEE WCNC'18 - LCEN Workshop*, April 2018.

[18] M. Petovello, K. Keefe, B. Chan, S. Spiller, C. Pedrosa, and P. Xie, "Demonstration of Inter-Vehicle UWB Ranging to Augment DGPS for Improved Relative Positioning," *Journal of GPS*, vol. 11, no. 1, pp. 11–21, 2012.

[19] http://hights.eu/. Accessed: 2018-06-30.

[20] N. Drawil and O. Basir, "Inter-vehicle Communication-Assisted Localization," *IEEE Trans. on ITS*, vol. 11, pp. 678–691, Sept. 2010.

[21] https://bespoon.com/. Accessed: 2018-06-30.

[22] S. Datta, M. Khan, L. Codeca, B. Denis, J. Härri, and C. Bonnet, "IoT and Microservices Based Testbed for Connected Car Services," in *Proc. IEEE SmartVehicles'18 - WoWMoM*, pp. 14–19, June 2018.